



A simple method for understanding the triangular growth patterns of transition metal dichalcogenide sheets

Siya Zhu and Qian Wang

Citation: *AIP Advances* **5**, 107105 (2015); doi: 10.1063/1.4933021

View online: <http://dx.doi.org/10.1063/1.4933021>

View Table of Contents: <http://scitation.aip.org/content/aip/journal/adva/5/10?ver=pdfcov>

Published by the [AIP Publishing](#)

Articles you may be interested in

[Enhancement of band-to-band tunneling in mono-layer transition metal dichalcogenides two-dimensional materials by vacancy defects](#)

Appl. Phys. Lett. **104**, 023512 (2014); 10.1063/1.4862667

[Charge conduction and relaxation in MoS₂ nanoflakes synthesized by simple solid state reaction](#)

J. Appl. Phys. **114**, 043710 (2013); 10.1063/1.4816570

[Controlled growth of vertically oriented molybdenum oxide nanoplates](#)

AIP Conf. Proc. **1536**, 35 (2013); 10.1063/1.4810087

[First-principles theoretical analysis of transition-metal doping of ZnSe quantum dots](#)

J. Appl. Phys. **112**, 024301 (2012); 10.1063/1.4734841

[Role of oxygen atoms in the growth of magnetron sputter-deposited ZnO films](#)

J. Appl. Phys. **108**, 033521 (2010); 10.1063/1.3457867

The advertisement features a blue and orange background with a molecular structure of blue spheres. On the left is a cover image of 'AIP Applied Physics Reviews' showing a diagram of a layered material. The main text reads 'NEW Special Topic Sections' in large white font. Below this, it says 'NOW ONLINE' in yellow, followed by 'Lithium Niobate Properties and Applications: Reviews of Emerging Trends' in white. The AIP Applied Physics Reviews logo is in the bottom right corner.

NEW Special Topic Sections

NOW ONLINE
Lithium Niobate Properties and Applications:
Reviews of Emerging Trends

AIP Applied Physics Reviews

A simple method for understanding the triangular growth patterns of transition metal dichalcogenide sheets

Siya Zhu^{1,2,3} and Qian Wang^{1,2,3,a}

¹Center for Applied Physics and Technology, College of Engineering, Peking University, Beijing 100871, China

²Key Laboratory of High Energy Density Physics Simulation, and IFSA Collaborative Innovation Center, Ministry of Education, Beijing 100871, China

³Department of Materials Science and Engineering, College of Engineering, Peking University, China

(Received 5 August 2015; accepted 28 September 2015; published online 7 October 2015)

Triangular nanoflake growth patterns have been commonly observed in synthesis of transition metal dichalcogenide sheets and their hybrid structures. Triangular nanoflakes not only show exceptional properties, but also can serve as building blocks for two or three dimensional structures. In this study, taking the MoS₂ system as a test case, we propose a Matrix method to understand the mechanism of such unique growth pattern. Nanoflakes with different edge types are mathematically described with configuration matrices, and the total formation energy is calculated as the sum of the edge formation energies and the chemical potentials of sulfur and molybdenum. Based on energetics, we find that three triangular patterns with the different edge configurations are energetically more favorable in different ranges of the chemical potential of sulfur, which are in good agreement with experimental observations. Our algorithm has high efficiency and can deal with nanoflakes in microns which are beyond the ability of *ab-initio* method. This study not only elucidates the mechanism of triangular nanoflake growth patterns in experiment, but also provides a clue to control the geometric configurations in synthesis. © 2015 Author(s). All article content, except where otherwise noted, is licensed under a Creative Commons Attribution 3.0 Unported License. [<http://dx.doi.org/10.1063/1.4933021>]

The novel physical and chemical properties of graphene, together with its technological applications¹ have stimulated considerable interest in the search of other two-dimensional (2D) materials. Among them, monolayer transition metal dichalcogenides (TMDs) have currently been in the focus due to their various novel electronic²⁻⁸ and optical⁹⁻¹¹ properties, and many promising applications in catalysis,¹² hydrogen storage,¹³ transistors,¹⁴ photovoltaic,¹⁵ and Li-ion batteries.¹⁶ Despite the variety of compositions and properties, all monolayer TMDs (MX₂, M = Mo, W, V; X = S, Se, Te) share an interesting common feature in structure, namely the nanoflakes of TMDs grow in triangular shapes varying in their edge compositions.^{17,18} For example, on Au substrate MoS₂ sheets grow in triangular shape with the edge length up to 115 μm,¹⁹ which has also been observed on single-crystalline sapphire (0001) substrates in chemical vapor deposition (CVD),²⁰ and these triangular nanoflakes can form three-dimensional spirals.²¹ Moreover, the intriguing triangular growth patterns have also been observed in MoS₂-WS₂ hybrid sheets.^{22,23} It has been found that the special triangular nanoflakes of TMDs exhibit many interesting physical and chemical properties.²⁴ This unique growth pattern inspires people to investigate the underlying reasons. Although density functional theory (DFT) based calculations²⁵ were carried out to understand the stability of triangular nanoflakes, the effect of edge configurations on the stability has not been studied yet. In addition, DFT calculation cannot deal with the nanoflakes in micron dimensions containing millions of atoms as observed in experiments.¹⁹

^aCorresponding author: qianwang2@pku.edu.cn



In this work, we develop a simple but effective Matrix method to understand the mechanisms of triangular growth patterns of TMDS. Taking the MoS₂ system as an example, we find that with different chemical potentials of sulfur, the triangular shaped MoS₂ nanoflakes with different edge configurations have much lower formation energy among all the nanoflakes with other shapes. Our results not only explain the experimental observations of triangular growth patterns and various edge types of MoS₂ nanoflakes, but also suggest an appropriate synthesis condition to control the edge configurations of nanoflakes.

Our DFT calculations were performed with the Vienna *ab-initio* simulation package (VASP)²⁰ at the level of the generalized gradient approximation (GGA) with the Perdew-Burke-Ernzerhof (PBE)²¹ exchange and correlation functional. The wave functions are expanded with a plane-wave basis set having a cutoff energy of 400 eV. For geometry optimization and total energy calculations of 2D MoS₂ nanosheets, a vacuum space of 20 Å is applied in the direction perpendicular to the sheet, and a k-mesh of 7 × 7 × 1 is used. While for MoS₂ nanoribbons, a vacuum space of 25 Å × 20 Å along the *y* and *z* directions is employed with a k-mesh of 7 × 1 × 1. For MoS₂ finite nanoflakes, a 20 Å × 20 Å × 20 Å supercell is used with a k-mesh of 1 × 1 × 1.

We first conducted geometry optimization for a perfect single-layer MoS₂ sheet, which is composed of the hexagonal honeycomb unit cells with one sulfur atomic layer on the top and bottom respectively, and one molybdenum atomic layer in the middle. The optimized structure has a lattice parameter of 3.184 Å, and the binding energy per MoS₂ unit is calculated to be $E_{\text{MoS}_2} = -21.797$ eV, which agrees well with previous experimental and theoretical results.^{22,23}

Four different types of edges that are commonly seen in single-layer MoS₂ nanoflakes are taken into account: zigzag-Mo edge, zigzag-S edge, antenna-S edge, and antenna-Mo edge, labeled as I, II, III, and IV, respectively, as shown in Fig. 1.

Based on the feature of honeycomb structural cell of 2D MoS₂ sheets and previous experimental findings of triangular and hexagonal MoS₂ nanoflakes, we consider the convex hexagonal nanoflakes with all angles of 120°, and the six edges in the different configurations shown in Fig. 1. We use a matrix to describe such a nanoflake. For instance, for the MoS₂ nanoflake shown in Fig. 2(a), the configuration matrix **X** can be expressed as

$$\mathbf{X} = \begin{pmatrix} 0 & 0 & 0 & 2 \\ 4 & 0 & 0 & 0 \\ 0 & 2 & 0 & 0 \\ 0 & 0 & 4 & 0 \\ 0 & 2 & 0 & 0 \\ 4 & 0 & 0 & 0 \end{pmatrix},$$

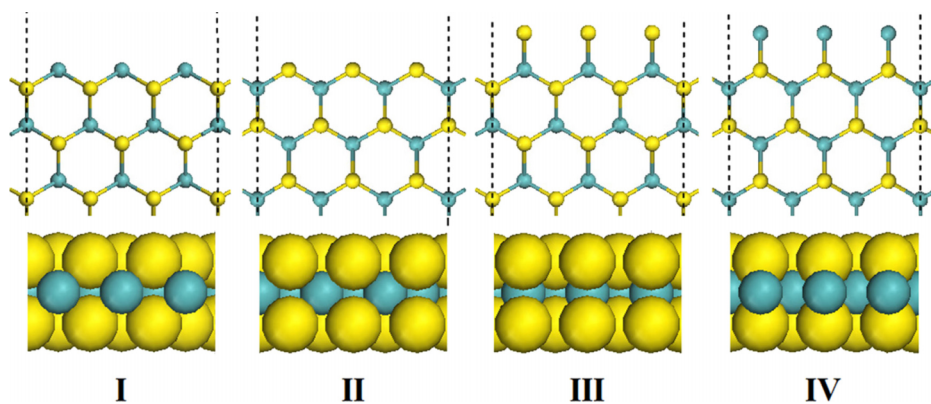


FIG. 1. Top and side views of the four different edge configurations of MoS₂ nanoflakes. Zigzag-Mo edge, zigzag-S edge, antenna-S edge, and antenna-Mo edge are labeled as I, II, III, and IV, respectively.

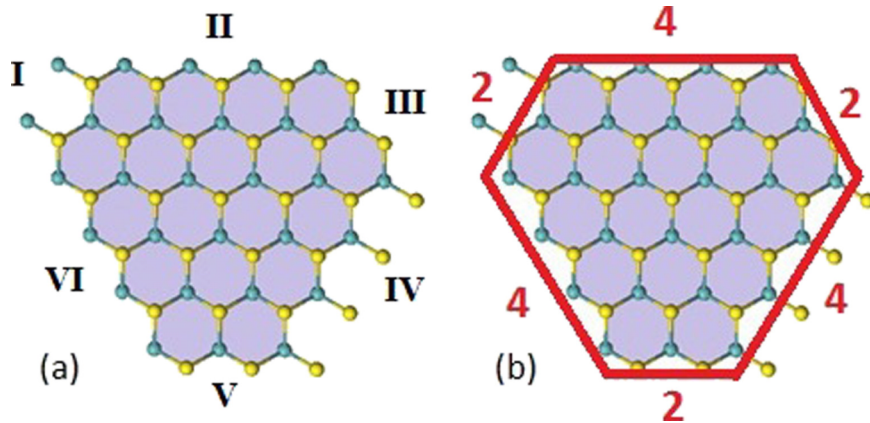


FIG. 2. (a) A MoS₂ nanoflake with convex hexagonal shape. Edges are numbered I to VI from the top-left edge, corresponding to the row in matrix. (b) Edge length of the hexagonal nanoflake.

where the four columns represent the four types of edges, and the six rows are for the edge length of the six edges characterized by the number of the honeycomb structural unit cells, starting from the top-left edge, as labeled in Figure 2(a).

In an infinite MoS₂ monolayer, one Mo atom is coordinated to six S atoms, and one S atom is coordinated to three Mo atoms, forming a stable structure. However, in a finite MoS₂ nanoflake, Mo atoms on the edges no longer have perfect triangular prismatic coordination, and S atoms on the edges no longer have perfect triangular pyramid coordination. Therefore, such unsaturated atoms on the edges would increase the free energy, which is termed as edge formation energy, acting as a controlling thermodynamical parameter in formation and growth of nanoflakes. The average edge formation energy per unit length of an edge (γ) is used to measure the stability of a nanoflake with different edge configurations, namely the lower γ , the lower total free energy, and more stable the nanoflake is.

To calculate parameter γ , we label the formation energy of the four types of the edges in Fig. 1 as γ_I , γ_{II} , γ_{III} and γ_{IV} , respectively, which is a function of the chemical potentials of sulfur and molybdenum. We define the edge formation energy vector Γ as

$$\Gamma = \begin{pmatrix} \gamma_I \\ \gamma_{II} \\ \gamma_{III} \\ \gamma_{IV} \end{pmatrix}. \quad (1)$$

Thus, the average edge formation energy can be expressed as

$$\gamma = \frac{\sum \mathbf{X} \cdot \Gamma}{\sum \mathbf{X}} \quad (2)$$

Therefore, the formation energy computed by DFT method in previous work²⁴ can be calculated now by the simple algebra equations in our Matrix method.

In order to find the formation energy of different edges, a common method is to calculate the total free energy of the nanoribbons with different edge configurations, and subtract the chemical potentials of the species in their corresponding 2D crystalline nanolayers.^{25,26}

For the MoS₂ nanoribbons with the different edge configurations constructed by the combination of the four edges, as shown in Fig. 3, we have

$$\gamma_I + \gamma_{II} = E_{I+II} - 6\mu_{Mo} - 12\mu_S \quad (3)$$

$$\gamma_{II} + \gamma_{III} = E_{II+III} - 6\mu_{Mo} - 14\mu_S \quad (4)$$

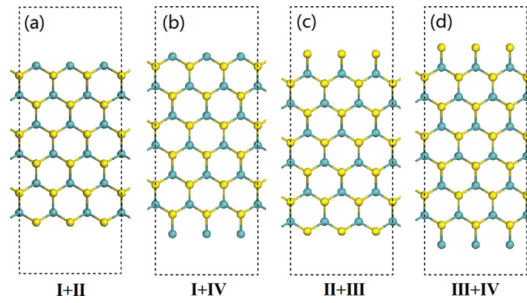


FIG. 3. MoS₂ nanoribbons with four different combinations of the typical edge configurations: (a) I+II, (b) I+IV, (c) II+III, and (d) III+IV.

$$\gamma_I + \gamma_{IV} = E_{I+IV} - 7\mu_{Mo} - 12\mu_S \quad (5)$$

$$\gamma_{III} + \gamma_{IV} = E_{III+IV} - 7\mu_{Mo} - 14\mu_S \quad (6)$$

where E is the total free energy of the nanoribbons, μ_{Mo} and μ_S are the chemical potentials of molybdenum and sulfur.

From Equation (3) to (6), we obtain that $E_{I+II} + E_{III+IV}$ equals $E_{I+IV} + E_{II+III}$.

While from DFT calculations, we get

$$E_{I+II} = -126.373 \text{ eV}$$

$$E_{II+III} = -137.067 \text{ eV}$$

$$E_{I+IV} = -135.956 \text{ eV}$$

$$E_{III+IV} = -146.695 \text{ eV}$$

Thus, $E_{I+II} + E_{III+IV} = -273.068 \text{ eV}$, and $E_{I+IV} + E_{II+III} = -273.023 \text{ eV}$, showing a good self-consistency of the equations.

Equations (3)-(6) derived from the nanoribbons are not enough to solve the formation energy of each edge, so that a triangular nanoflake with the shape characterized by the configuration matrix:

$$\mathbf{X} = \begin{bmatrix} 0 & 3 & 0 & 0 \\ 0 & 0 & 1 & 0 \\ 0 & 3 & 0 & 0 \\ 0 & 0 & 1 & 0 \\ 0 & 3 & 0 & 0 \\ 0 & 0 & 1 & 0 \end{bmatrix}$$

is computed to provide another equation:

$$\begin{bmatrix} 0 & 3 & 0 & 0 \\ 0 & 0 & 1 & 0 \\ 0 & 3 & 0 & 0 \\ 0 & 0 & 1 & 0 \\ 0 & 3 & 0 & 0 \\ 0 & 0 & 1 & 0 \end{bmatrix} \begin{pmatrix} \gamma_I \\ \gamma_{II} \\ \gamma_{III} \\ \gamma_{IV} \end{pmatrix} = 9\gamma_{II} + 3\gamma_{III} = E_{9II+3III} - 10\mu_{Mo} - 30\mu_S \quad (7)$$

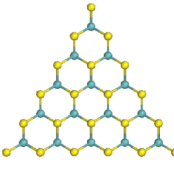
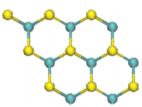
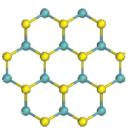
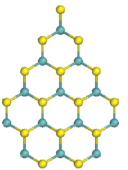
With DFT calculations, we get the binding energy of the nanoflake: $E_{9II+3III} = -245.931 \text{ eV}$.

In an equilibrium growth and annealing condition of MoS₂ nanoflakes, we have

$$\mu_{MoS_2} = \mu_{Mo} + 2\mu_S \quad (8)$$

which equals to the energy of a unit cell of MoS₂ nanosheet, namely -21.797 eV .

TABLE I. Total energy E_{total} (in eV) and edge formation energy γ (in eV) of the four typical shaped MoS₂ nanoflakes calculated by DFT and our matrix method.

Shape	X matrix	DFT computation		Matrix method	
		E_{total}	γ	E_{total}	γ
	$\begin{bmatrix} 0 & 4 & 0 & 0 \\ 0 & 0 & 1 & 0 \\ 0 & 4 & 0 & 0 \\ 0 & 0 & 1 & 0 \\ 0 & 4 & 0 & 0 \\ 0 & 0 & 1 & 0 \end{bmatrix}$	-359.288	$-2.136 - \frac{4}{3}\mu_S$	-359.460	$-2.167 - \frac{4}{3}\mu_S$
	$\begin{bmatrix} 0 & 0 & 1 & 0 \\ 0 & 2 & 0 & 0 \\ 2 & 0 & 0 & 0 \\ 0 & 1 & 0 & 0 \\ 2 & 0 & 0 & 0 \\ 0 & 2 & 0 & 0 \end{bmatrix}$	-162.730	$1.164 - \frac{1}{3}\mu_S$	-163.015	$1.138 - \frac{1}{3}\mu_S$
	$\begin{bmatrix} 0 & 2 & 0 & 0 \\ 2 & 0 & 0 & 0 \\ 0 & 2 & 0 & 0 \\ 2 & 0 & 0 & 0 \\ 0 & 2 & 0 & 0 \\ 2 & 0 & 0 & 0 \end{bmatrix}$	-234.789	2.231	-235.098	2.201
	$\begin{bmatrix} 0 & 3 & 0 & 0 \\ 0 & 0 & 1 & 0 \\ 0 & 3 & 0 & 0 \\ 2 & 0 & 0 & 0 \\ 0 & 2 & 0 & 0 \\ 2 & 0 & 0 & 0 \end{bmatrix}$	-277.803	$0.428 - \frac{4}{13}\mu_S$	-276.554	$0.524 - \frac{4}{13}\mu_S$

With Equations (3)-(8), the formation energy of each edge can be solved as following:

$$\begin{aligned}\gamma_I &= 5.929 \text{ eV} + \frac{2}{3}\mu_S \\ \gamma_{II} &= -1.518 \text{ eV} - \frac{2}{3}\mu_S \\ \gamma_{III} &= -4.765 \text{ eV} - \frac{4}{3}\mu_S \\ \gamma_{IV} &= 10.696 \text{ eV} + \frac{4}{3}\mu_S\end{aligned}$$

In CVD process, the chemical potential of sulfur changes in the range of $-5.4 \text{ eV} \sim -3.8 \text{ eV}$.²⁴ To examine the accuracy of our method, the formation energy of four typical shaped MoS₂ nanoflakes (triangle, parallelogram, hexagon, and pear) were calculated by both DFT and our Matrix method. The calculated results are given in Table I, which shows that the results provided by Matrix method are in good agreement with those obtained by DFT, confirming the accuracy of our method.

With the different chemical potential of sulfur μ_S , the formation energies of the edges change gradually, as shown in Figure 4(d). Hence, different shapes of nanoflakes are determined by the energetics. Based on Figure 4(d), we can clearly see that antenna-Mo edge configuration is energetically most unfavorable, while the relative stability of other three edge configurations depends on the chemical potential of S, which can be discussed in the three ranges: $-5.4 \text{ eV} < \mu_S < -5.347 \text{ eV}$, $-5.347 \text{ eV} < \mu_S < -4.871 \text{ eV}$, and $-4.871 \text{ eV} < \mu_S < -3.8 \text{ eV}$, controlling the formation energy of nanoflakes with different edge configurations.

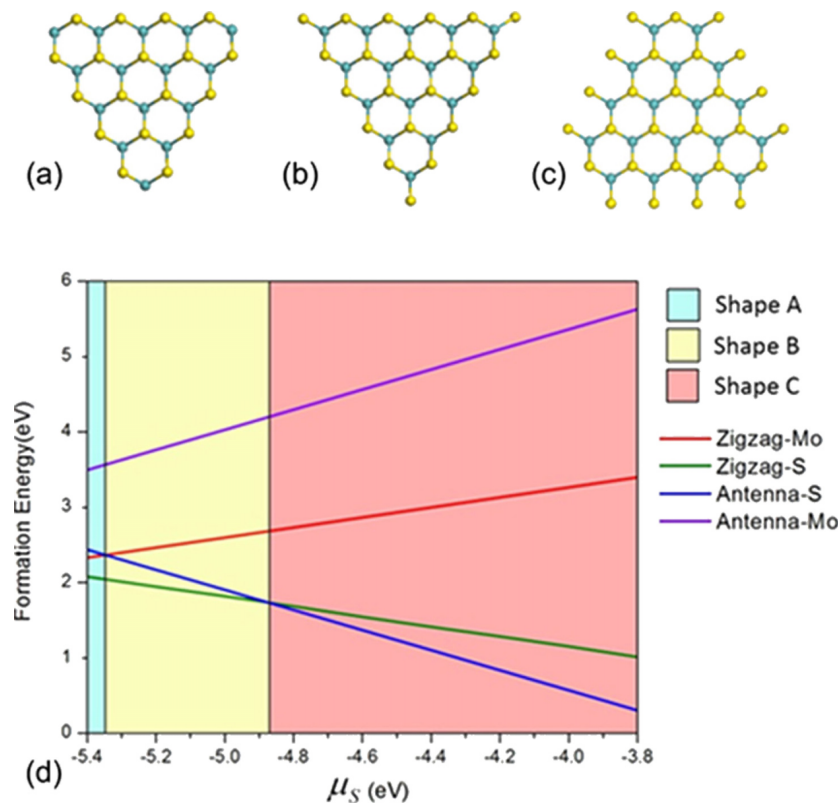


FIG. 4. (a), (b), and (c) Geometries of the three thermodynamically stable triangular nanoflakes. (d) Variation of the edge formation energy with respect to the chemical potential of sulfur μ_S for the triangular nanoflakes with different edge configurations.

$$(i) -5.4 \text{ eV} < \mu_S < -5.347 \text{ eV}$$

Under this condition, the stability follows the order of zigzag-S edge > zigzag-Mo edge > antenna-S edge. However, a hexagonal MoS₂ nanoflake cannot be formed with zigzag-S edges merely. In fact, at least three alternated edges should be either zigzag-Mo edges or antenna-S edges. Therefore, the thermodynamically most stable structure within such μ_S range should be in a triangular nanoflake, with three zigzag-S edges as long as possible, and three zigzag-Mo edges as short as possible, as shown in Fig. 4(a), named shape A.

$$(ii) -5.347 \text{ eV} < \mu_S < -4.871 \text{ eV}$$

In this range, Fig. 4(d) shows that the zigzag-S edge configuration is more stable than the antenna-S edge one, which is in turn energetically preferable than the zigzag-Mo edge configuration. Therefore the most thermodynamically stable structure should also be in a triangular shape, with three zigzag-S edges as long as possible, and three antenna-S edges as short as possible, as shown in Fig. 4(b), named shape B.

$$(iii) -4.871 \text{ eV} < \mu_S < -3.8 \text{ eV}$$

In this case, the antenna-S edges have the lowest formation energy, and then the zigzag-S edges. Therefore the most thermodynamically stable structure should still be in a triangular shape, with three antenna-S edges as long as possible, and three zigzag-S edges as short as possible, as shown in Figure 4(c), named shape C.

Based on above discussions, three thermodynamically stable configurations are identified for different μ_S , and all of them have triangular shape with favorable formation energy. This is the reason why triangular growth patterns have been observed in many experiments.^{9,17} However, when

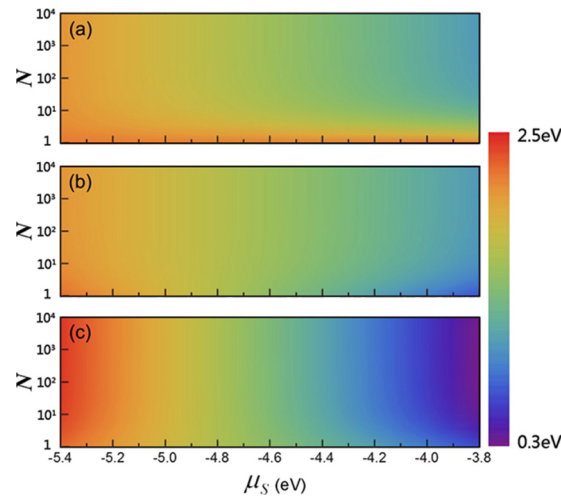


FIG. 5. Variation of the average edge formation energy with respect to the edge length N and chemical potential μ_S for MoS₂ nanoflakes in shape A (a), B (b) and C (c).

μ_S is about -4.871 eV, the formation energies of the zigzag-S edges and antenna-S edges are comparable. Therefore, growth of six edges of the hexagonal MoS₂ has no priority, and orthohexagonal nanoflakes of MoS₂ can be synthesized in such special chemical condition. Recently, the Wang group reported the synthesis of such hexagonal MoS₂ nanoflake experimentally.²⁷

To simulate the configuration evolution during the growth from small to large size in microns for these three stable triangular structures, we study the relationship among γ (average edge formation energy per unit length of the edge), N (the edge length, characterizing by the number of hexagonal unit cells in the edge), and μ_S (the chemical potential of S). The calculated results for the triangular nanoflakes in shape A, B and C are plotted in Fig. 5(a), 5(b) and 5(c), respectively, where the color with scale bar represents edge formation energy. The Figure shows that the average edge formation energies of shape A and C become smaller when the size N is getting larger. For shape B, when $\mu_S < -4.871$ eV, γ decreases with N ; when $\mu_S > -4.871$ eV, γ increases with N . In other words, in a Mo-rich environment, all three shapes have tendencies to grow thermodynamically, while in a S-rich environment, the growth of shape A and C to large size is preferable but not for shape B. The Lauritsen group¹⁸ reported that shape B only exists in the nanoflakes with edge length less than 5, and big nanoflakes are practically in shape C. Based on above discussions, we conclude that the synthesis of nanoflakes in shape A and C should be in a S-rich condition, where the growth of nanoflakes in shape B is unfavorable, while shape C is thermodynamically favorable.

In summary, we propose a Matrix method to calculate the edge formation energy of nanoflakes where the configuration of nanoflakes is described with a matrix, and the total formation energy is approximated to be the sum of edge formation energies and the chemical potentials of sulfur and molybdenum. We have identified three thermodynamically stable triangular shapes with different edge configurations for MoS₂ nanoflakes which are controlled by the chemical potentials of sulfur and molybdenum. In a Mo-rich synthesis condition, shape A and B are preferable, while in a S-rich synthesis environment, shape C is more favorable. Our Matrix method not only provides the results that agree well with those obtained from DFT calculations, but also it is beyond DFT as it can deal with large nanoflakes in microns containing millions of atoms as observed in experimental synthesis. Furthermore, we can extend the matrix method to other transition metal dichalcogenide nanoflakes like WS₂.²⁸

ACKNOWLEDGEMENTS

This work is partially supported by grants from the National Natural Science Foundation of China (NSFC-11174014, NSFC-51471004), the National Grand Fundamental Research 973

Program of China (Grant No. 2012CB921404), and the Doctoral Program of Higher Education of China (20130001110033).

- ¹ Andre K. Geim and Konstantin S. Novoselov, *Nat. Mater.* **6**(3), 183 (2007).
- ² Mehmet Topsakal and Salim Ciraci, *Phys. Rev. B* **85**(4), 045121 (2012).
- ³ Viktoria V. Ivanovskaya, Alberto Zobelli, Alexandre Gloter, Nathalie Brun, Virginie Serin, and Christian Colliex, *Phys. Rev. B* **78**, 134104 (2008).
- ⁴ S. Lebegue and O. Eriksson, *Phys. Rev. B* **79**, 115409 (2009).
- ⁵ Agnieszka Kuc, Nourdine Zibouche, and Thomas Heine, *Phys. Rev. B* **83**, 245213 (2011).
- ⁶ Ashwin Ramasubramaniam, Doron Naveh, and Elias Towe, *Phys. Rev. B* **84**, 205325 (2011).
- ⁷ R. H. Friend and A. D. Yoffe, *Adv. Phys.* **36**, 1 (1987).
- ⁸ Yandong Ma, Ying Dai, Wei Wei, Chengwang Niu, Lin Yu, and Baibiao Huang, *J. Phys. Chem. C* **115**, 20237 (2011).
- ⁹ Tsegabirhan B. Wendumu, Gotthard Seifert, Tommy Lorenz, Jan-Ole Joswig, and Andrey Enyashin, *J. Phys. Chem. Lett.* **5**, 3636 (2014).
- ¹⁰ Qingqing Ji, Yanfeng Zhang, Teng Gao, Yu Zhang, Donglin Ma, Mengxi Liu, Yubin Chen, Xiaofen Qiao, Ping-Heng Tan, and Min Kan, *Nano Lett.* **13**, 3870 (2013).
- ¹¹ Humberto R. Gutiérrez, Nestor Perea-López, Ana Laura Elías, Ayse Berkdemir, Bei Wang, Ruitao Lv, Florentino López-Urías, Vincent H. Crespi, Humberto Terrones, and Mauricio Terrones, *Nano Lett.* **13**, 3447 (2012).
- ¹² Yanguang Li, Hailiang Wang, Liming Xie, Yongye Liang, Guosong Hong, and Hongjie Dai, *J. Am. Chem. Soc.* **133**, 7296 (2011).
- ¹³ Jun Chen, Nobuhiro Kuriyama, Huatang Yuan, Hiroyuki T. Takeshita, and Tetsuo Sakai, *J. Am. Chem. Soc.* **123**, 11813 (2001).
- ¹⁴ Branimir Radisavljevic, Aleksandra Radenovic, Jacopo Brivio, V. Giacometti, and A. Kis, *Nat. Nanotechnol.* **6**, 147 (2011).
- ¹⁵ Marcio Fontana, Tristan Deppe, Anthony K. Boyd, Mohamed Rinzan, Amy Y. Liu, Makarand Paranjape, and Paola Barbara, *Sci. Rep.* **3**, 1634 (2013).
- ¹⁶ Kun Chang and Weixiang Chen, *J. Mater. Chem.* **21**, 17175 (2011).
- ¹⁷ S. Helveg, Jeppe Vang Lauritsen, Erik Lægsgaard, Ivan Stensgaard, Jens Kehlet Nørskov, B. S. Clausen, H. Topsøe, and Flemming Besenbacher, *Phys. Rev. Lett.* **84**, 951 (2000).
- ¹⁸ J. V. Lauritsen, J Kibsgaard, S Helveg, H Topsøe, B. S. Clausen, E Laegsgaard, and F Besenbacher, *Nat. Nanotechnol.* **2**, 53 (2007).
- ¹⁹ Yi Hsien Lee, Xin Quan Zhang, Wenjing Zhang, MuTung Chang, Cheng Te Lin, Kai Di Chang, Ya Chu Yu, Jacob TseWei Wang, Chia Seng Chang, and LainJong Li, *Adv. Mater.* **24**, 2320 (2012).
- ²⁰ G. Kresse and J. Furthmuller, *Phys. Rev. B* **54**, 11169 (1996).
- ²¹ J. P. Perdew, K. Burke, and M. Ernzerhof, *Phys. Rev. Lett.* **77**, 3865 (1996).
- ²² C. Ataca and S. Ciraci, *J. Phys. Chem. C* **115**, 13303 (2011).
- ²³ D. Yang, S. Jiménez Sandoval, W. M. R. Divigalpitiya, J. C. Irwin, and R. F. Frindt, *Phys. Rev. B* **43**, 12053 (1991).
- ²⁴ Yungang Zhou, Ping Yang, Haoyue Zu, Fei Gao, and Xiaotao Zu, *Phys. Chem. Chem. Phys.* **15**, 10385 (2013).
- ²⁵ Yuanyue Liu, Somnath Bhowmick, and Boris I. Yakobson, *Nano Lett.* **11**, 3113 (2011).
- ²⁶ Sukky Jun, *Phys. Rev. B* **78**, 073405 (2008).
- ²⁷ Shanshan Wang, Youmin Rong, Ye Fan, Mercè Pacios, Harish Bhaskaran, Kuang He, and Jamie H. Warner, *Chem. Mat.* **26**, 6371 (2014).
- ²⁸ See supplementary material at <http://dx.doi.org/10.1063/1.4933021> for WS₂ growth pattern calculated with matrix method.